Deep-Sea Research II 58 (2011) 1384–1391

Contents lists available at ScienceDirect

Deep-Sea Research II

journal homepage: www.elsevier.com/locate/dsr2

^{234}Th-Based Carbon Export around Free-Drifting Icebergs in the Southern Ocean

T.J. Shaw [1,*], K.L. Smith Jr.[2], C.R. Hexel [1], Rebekkah Dudgeon [1], Alana D. Sherman [2], M. Vernet [3], R.S. Kaufmann [4]

[1] Department of Chemistry and Biochemistry, University of South Carolina, 931 Sumter Street Columbia, SC 29208, USA
[2] Monterey Bay Aquarium Research Institute, 7700 Sandholdt Road, Moss Landing, CA 95039, USA
[3] Marine Biology Research Division, Scripps Institution of Oceanography, University of California, San Diego, La Jolla, CA 92093-0202, USA
[4] Marine Science and Environmental Studies Department, University of San Diego, 5998 Alcalá Park, San Diego, CA 92110-2492, USA

ARTICLE INFO

Article history:
Received 12 November 2010
Accepted 12 November 2010
Available online 21 December 2010

Keywords:
Iron fertilization
Carbon sequestration
Carbon export efficiency
Atmospheric carbon drawdown

ABSTRACT

The impact of free-drifting icebergs on the efficiency of carbon export from the upper water column was measured using the disequilibrium of ^{234}Th and its parent ^{238}U. The study addressed the null hypothesis that free-drifting icebergs do not alter ^{234}Th deficiency and carbon export compared to surrounding waters. Upper-water-column inventories of ^{234}Th were measured at six stations in the Weddell Sea concurrently with four deployments of Lagrangian Sediment Traps (LSTs) during a cruise in March/April 2009. Four stations were sampled ranging from 0.3 km to <20 km of the edge of a large free-drifting iceberg (C-18a) and two were sampled at distances >60 km from C-18a. Temperature and salinity anomalies indicated enhanced upwelling and turbulent mixing extending downstream of the iceberg to a minimum of $\sim$20 km from the iceberg edge. Separate studies of the impact of C-18a on water column physical properties were used to define the extent of the iceberg's influence on surrounding waters.

The largest upper-water-column deficiencies in the inventories of ^{234}Th were measured in close proximity and downstream of the iceberg and extending to below 100 m depth. A steady-state model was used to estimate the export of ^{234}Th from the upper water column. Organic carbon export was calculated using C/Th from the concurrent LST collections. Comparison of stations within the iceberg's influence (close proximity and downstream to within 20 km of the iceberg) and far-field (greater than 60 km) measurements showed a factor of 3 increase in organic carbon export near the iceberg. The factor correlated well with the results from the near- and far-field LST measurements. Differences in the magnitude of carbon export at 100 and 600 m indicate that $\sim$90 percent of the exported material is regenerated by 600 m depth. This study confirms that the increased abundance of large free-drifting icebergs in the Southern Ocean can contribute to the drawdown of atmospheric CO_2 through increased organic carbon export.

1. Introduction

A dramatic increase in ice loss and the associated release of icebergs from Antarctica (Stuart and Long, 2011) has the potential to contribute to atmospheric carbon drawdown in the Southern Ocean. Free-drifting icebergs have been shown to harbor an enriched biological community compared to regions of low productivity that characterize the Southern Ocean (Smith et al., 2007). The enrichment of biological activity associated with free-drifting icebergs may provide a negative feedback to increased warming through enhanced carbon export from surface waters and associated drawdown of atmospheric CO_2. One likely contribution to this enriched community is the release of micronutrient iron as icebergs ablate (Martin et al., 1990; de Baar et al., 1995; Raiswell et al., 2006; 2008; Smith et al., 2007; Lin et al., 2011; Shaw et al., 2011). Chemical forcing of enriched primary production has been well established through iron fertilization experiments in the Southern Ocean (de Baar et al., 2005). Similarly, the associated fertilization of primary productivity is expected to increase organic carbon export (Boyd, 2008). However, fertilization experiments cannot elucidate the function of a mature community on carbon export efficiency or the physical and chemical impact of large icebergs. The chemical forcing of community development is evident in regions of natural iron fertilization in the Southern Ocean (e.g., upwelling or island effects) and is thought to lead to enhanced carbon export (Pollard et al., 2009). Characteristics of these communities that may enhance carbon export include biological and physical factors in addition to nutrient inputs. Enhanced turbulence in proximity to a large tabular iceberg has been shown to increase local upwelling (Stephenson et al., 2011)

* Corresponding author.
E-mail address: shaw@chem.sc.edu (T.J. Shaw).

0967-0645/$ - see front matter © 2011 Elsevier Ltd. All rights reserved.
doi:10.1016/j.dsr2.2010.11.019

potentially increasing nutrient delivery to the upper water column. Phytoplankton community size effects associated with increased upwelling as well as increased carbon turnover through grazing and packaging by zooplankton and micronekton are known to contribute to elevated carbon export (Ebersbach and Trull, 2008). These factors, present in waters surrounding free-drifting icebergs, should result in enhanced carbon export in areas affected by icebergs (Smith et al., 2007).

The impact of free-drifting icebergs on phytoplankton community is indicated by the elevated abundance of larger cells near icebergs, with a general decrease in size with distance (Smith et al., 2007; Vernet et al., 2011). The abundance of large diatoms in close proximity to free-drifting icebergs is attributed to both enhanced local mixing and nutrient availability (Vernet et al., 2011). This is consistent with evidence that large-cell abundance is controlled by chemical and physical processes (Smith and Lancelot, 2004). Phytoplankton cell size has been shown to have a positive impact on sedimentation and, ultimately, carbon export efficiency (Bienfang, 1984; Buesseler, 1998). This has been attributed to factors such as resistance to predation and formation of fast-sinking aggregates associated with diatom blooms (Buesseler, 1998; Shaw et al., 1998). Material collected by Lagrangian Sediment Traps (LST's) in proximity to a large free-drifting iceberg (C-18a) contained abundant large and small diatoms as well as detrital aggregates (Smith et al., 2011).

Material collected in LST's near C-18a also contained abundant fecal material from grazers, indicating additional community control on phytoplankton population and carbon export. Icebergs also provide shelter and physical structure that furnish additional support for the grazer community (Smith et al., 2007; Sherlock et al., 2011; Kaufmann et al., 2011). Antarctic krill (*Euphausia superba*) are especially abundant within a few km of free-drifting icebergs (Smith et al., 2007; Kaufmann et al., 2011). Krill preferentially graze diatoms and cells $>10\,\mu m$ (Quetin and Ross, 1985) and are expected to exert significant population control (Walsh et al., 2001) as well as promoting carbon export as fecal material.

The use of water-column deficiency of ^{234}Th as a proxy for organic carbon export has been validated in numerous studies, including many in the Southern Ocean (Cochran et al., 2000; Savoye et al., 2008; Morris et al., 2007). The application is based on the near-constant production of ^{234}Th in the water column by the decay of its conservative parent ^{238}U and the strong partitioning of ^{234}Th onto solid phases. In most open-ocean environments, ^{234}Th is primarily partitioned onto biogenic material, thus its removal is proportional to the export of biogenic material. However, the partition coefficient of ^{234}Th varies with composition and size of the particulate phases (Buesseler et al., 2006), thus partitioning must be determined on local populations of particles, either by sediment trap collections or large-volume particulate collections. In this study, ^{234}Th deficiency is used as a proxy of organic carbon export to help validate concurrent sediment trap studies and elucidate mechanisms of carbon export in this unique community. We test the null hypothesis that large free-drifting icebergs have no measurable impact on ^{234}Th and organic carbon export from surface waters of the Northwestern Weddell Sea.

2. Methods

Water-column samples for ^{234}Th inventories were collected in late March and early April 2009 on a cruise to the Weddell Sea aboard the RVIB *Nathaniel B. Palmer*. A large tabular iceberg, C-18a, was located and tracked in the Powell Basin as the focus of the study (Fig. 1). The iceberg had dimensions of ~35 km length and ~6 km width and followed a clockwise movement around the basin (Helly et al., 2011). The study was conducted far from the seasonal ice edge to ensure that artifacts associated with ice borne algae (after Rodriguez y Baena et al., 2008) did not influence our ^{234}Th activity inventories. Water-column samples were collected in proximity to, and far-field from the iceberg during the course of the study (Fig. 1B) concurrent with four deployments of Lagrangian Sediment Traps (Smith et al., 2011). Samples were collected in Niskin bottles attached to a CTD rosette for the evaluation of ^{234}Th and organic carbon export from the upper water column. Additional water samples were collected for concurrent measurements of nutrients, plankton community, and bacterial activity for separate studies (Vernet et al., 2011, Murray et al., 2011).

The samples for ^{234}Th analysis were processed following the procedure of Pike et al. (2005) and Rutgers van der Loeff et al. (2006).

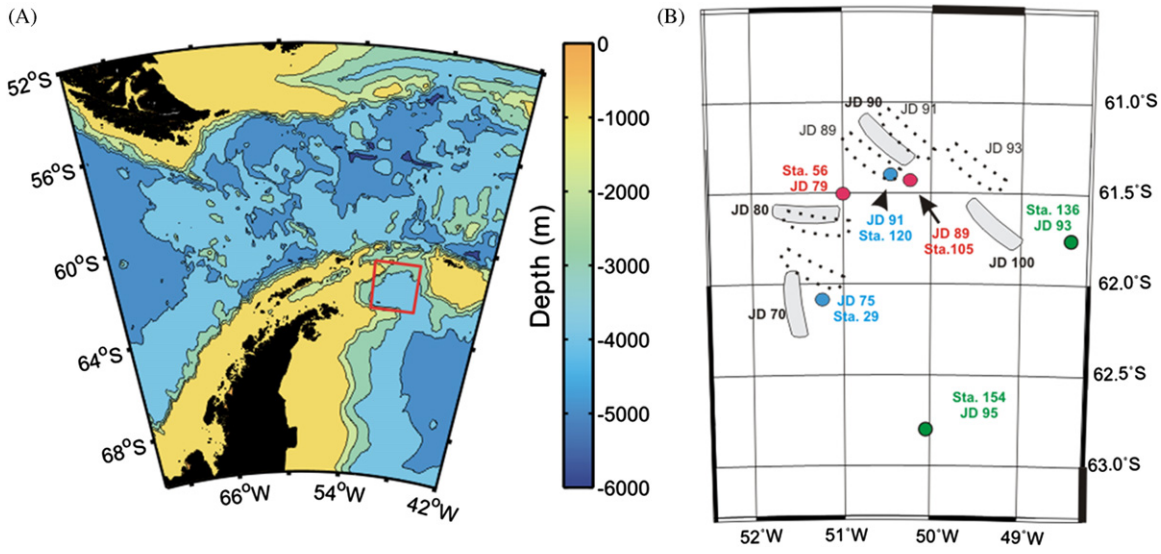

Fig. 1. (A) shows the study area in the Powell Basin of the Weddell sea. (B) shows the water column stations in relation to the iceberg position at the time of collection. Red water column station markers indicate positions downstream of the iceberg (at the time of collection), blue markers were positions upstream of the iceberg, and green markers were far-field stations. The solid iceberg markers represent well known positions based on circumnavigations (Helly et al., 2011), the dashed iceberg markers represent estimated positions at the time of sample collections. Note the general clockwise movement of iceberg C-18a around the basin.

Unfiltered 4-liter samples were collected from CTD mounted Niskin bottles and acidified to ~pH-2 within 1 hour of collection with HNO_3. Following acidification, a spike of ^{230}Th was added to each bottle as a yield monitor. Samples were allowed to equilibrate for a minimum of 12 hours and then the pH was adjusted to ~8 with concentrated NH_4OH. $KMnO_4$ and $MnCl_2$ solutions were added to co-precipitate the ambient ^{234}Th and the added ^{230}Th. The samples were allowed to stand for 12 hours and the precipitate was then filtered onto 25 mm-diameter Whatman QMA filters. Filters were allowed to dry and were then covered with 1 layer of Mylar sheet and mounted on filter holders for counting.

Organic carbon to ^{234}Th ratios were determined on five samples collected by free-drifting Lagrangian Sediment Traps (LST). The LST deployments lasted 3–4 days and samples were collected at 600 m depth for all deployments. No sample preservative was used during the short deployments (Smith et al., 2011). Splits from the LST were filtered onto pre combusted GMA filters, allowed to dry, and covered with 1 layer of Mylar sheet and mounted on filter holders as above.

Water-column and LST samples were counted for ^{234}Th beta emission on Risø counters within 4 days of collection. Total count times at sea were selected to yield total counts of greater than 3000, typically 1200 minutes for the water-column samples, resulting in first count errors of $<2\%$. Higher activities in the LST samples resulted in higher counts and lower errors (typically $\leq 1\%$) for the first count. Samples were returned to the laboratory and counted a second time at least 5 months after collection. Count time was selected to yield total counts of >1000 for the second counts to yield errors of $\leq 3\%$. However, in some cases counts were as low as 800 to yield second count errors of up to 3.5%.

After the second counts, filters containing LST samples were demounted, weighed, divided into two sections, reweighed, and placed in pre-combusted glass vials and shipped to the MSI Analytical Lab (Marine Science Institute, University of California, Santa Barbara, CA 93106) for CHN analysis. Water column samples were demounted from sample holders and placed in 15 ml vials for digestion. A ^{229}Th isotope dilution spike was added to each vial. The MnO_x precipitate was then digested by the addition of 8 N HNO_3 and H_2O_2. The sample and solution were sonicated for 20 minutes and allowed to sit overnight. Separation columns of AG X8 resin were prepared in a clean hood with 2 ml of resin and cleaned with repeated rinses of 12 N HCl. The resin was converted to the nitrate form by flushing with 8 N HNO_3, and the samples were loaded onto columns. Columns were rinsed with 8 HNO_3, and the Th was eluted with 9 N HCl. The eluent was collected in Teflon vials and dried on a hot plate in a clean hood. Samples were taken up in 1 ml of 8 N HNO_3, diluted to 4 ml for analysis by HR-ICP-MS (after Shaw and François, 1991).

The errors associated with analysis of ^{230}Th for recovery determinations included the uncertainty in the spike additions (both the recovery spike and the isotope dilution spike) and instrumental error. The recovery error was ~4%. However, five samples were collected at 2000 m at a 3000 meter depth site to measure procedural consistency for the method and to calculate counter efficiencies. The samples were counted twice within 5 days of collection, using different detector positions for the second counts. The overall standard deviation for the recovery corrected ^{234}Th activity in the five samples was 2%. While the calculated errors are significantly larger than the precision of the deep sample measurements, we have chosen to report a more conservative estimate of uncertainty. The error for ^{234}Th export is estimated at $\pm 8\%$, with pooled error for organic carbon export at $\pm 10\%$. In general, the calculated error is small compared to the range in measured values for organic carbon export. The water-column ^{238}U activity was assumed to be conservative and calculated from water-column salinity (after Chen et al., 1986).

Physical properties collected by CTD during sample collections were used to evaluate the area of physical influence of the iceberg (after Stephenson et al., 2011). TS plots for all water column collections (not shown) were used to verify common water mass characteristics below the maximum depth of iceberg C-18a (in the permanent thermocline).

3. Results

Inventories of ^{234}Th activity were measured for six water-column profiles in conjunction with deployments of Lagrangian Sediment Traps over a period of three weeks. Four profiles were collected near-field to iceberg C-18a (within 0.3, 3, and two at ~20 km), and two were collected in the far-field, greater than 60 km from C-18a (Fig. 1B). Two of the near-field stations (Sta. 56 and Sta. 105, 20 and 0.3 km, respectively) were collected downstream of the iceberg (in the path of iceberg movement). Two were collected up stream of the iceberg (Sta. 29 and Sta. 120, 3 and 20 km, respectively) (Fig. 1B). Water-column temperature and salinity (T and S) measurements confirmed a zone of physical impact (as upwelling of saltier "winter water" and broadening of the temperature minimum) downstream of the iceberg (Fig. 2, Sta. 56 and Sta. 105). It is important to point out that Sta. 105 and Sta. 120 were collected very close to each other in position (Fig. 1B). However due to iceberg movement between collections, Sta. 105 was sampled downstream of the iceberg and Sta. 120 was sampled upstream. While, the Sta. 29 CTD was taken near-field to the C-18a, the only physical evidence of iceberg influence is the smoothed transition in the upper mixed layer T and S profiles (Fig. 2).

Transmissivity and fluorescence were measured in the water column as proxies for particulate loading and chlorophyll concentration. Comparison of the upstream and downstream stations collected in proximity to the iceberg showed reduced transmissivity downstream of the iceberg in the surface mixed layer and (to a lesser extent) below (Fig. 3A). The <3-km upstream site (Sta. 29) lies between the downstream sites and the highest mixed layer transmissivity (lowest particle abundance), observed in the upstream station collected ~20-km from the iceberg. The plots of fluorescence (Fig. 3B) show a shallower fluorescence maximum in the two downstream sites (Sta. 56 and Sta. 105) and the <3-km upstream site (Sta. 29). This is consistent with shoaling of the upper mixed layer in the iceberg influenced water column (after Helly et al., 2011). There is also a clear deep (100–150 m) fluorescence signal in the downstream station collected closest to the iceberg (Sta. 105). The zone of deep fluorescence coincides with the zone of enhanced mixing indicated in the T and S profiles (Fig. 2). The transmissivity and fluorescence data show a clear "downstream" influence, with absolute proximity showing an observable but weaker influence.

Inventories of ^{234}Th activity were depleted by up to 30% with respect to the parent ^{238}U activity in the surface mixed layer (upper 30–50 m) of the water column in all six profiles (Fig. 4). The two near-field station profiles collected closest to C-18a and the downstream station at ~20 km showed deficiency below 100 m (Fig. 4A-C). Activities reached equilibrium with ^{238}U at or above 100 m for the upstream near-field station and the two far-field stations (Fig. 4D-F). Further, these stations all showed ^{234}Th regeneration by 100 m depth. In contrast, the near-field profiles and downstream stations showed no significant release of ^{234}Th directly below the photic zone for the depths measured (Fig Fig. 4A-C).

The station furthest from the iceberg position (Sta. 154) was collected in Iceberg Alley, a region where a number of small icebergs were present. There was no evidence of increased physical mixing in the region (Fig. 2). The ^{234}Th activity profile for the iceberg alley station showed the lowest deficiency in the surface

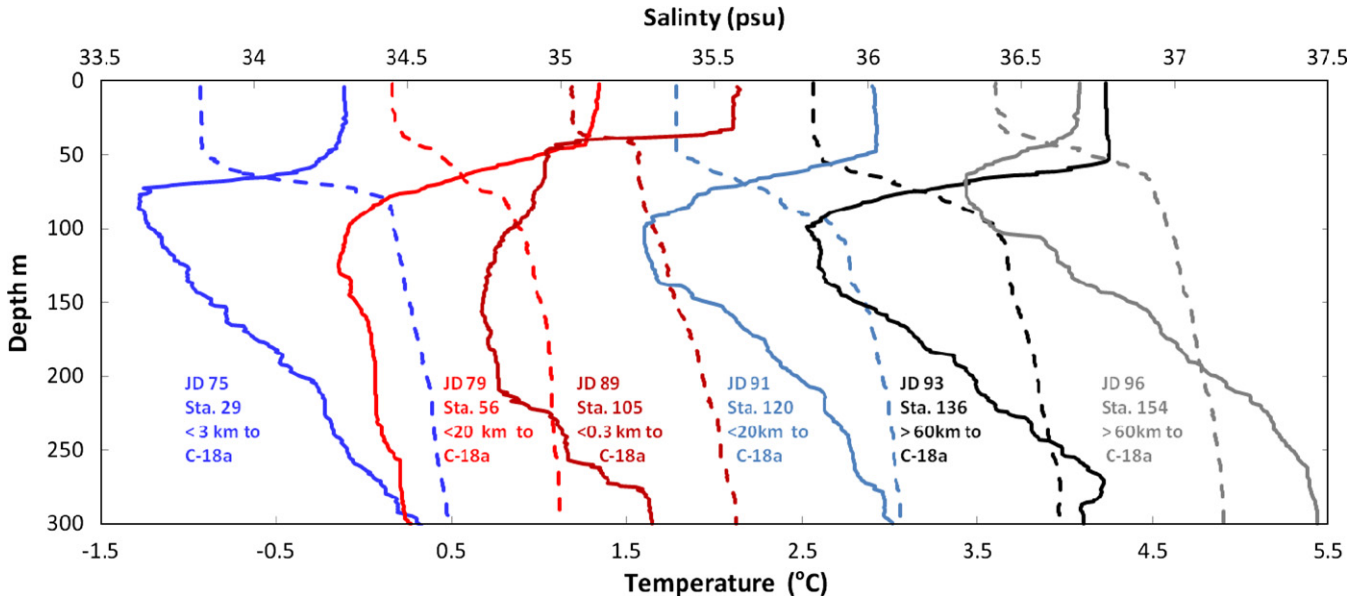

Fig. 2. Shows the upper water column temperature (T) and salinity (S) profiles as a time sequence starting 2 days before the first LST deployment and ending coincident with the last deployment. The T profiles are offset 1.0°C and the S profiles are offset 0.5 PSU.

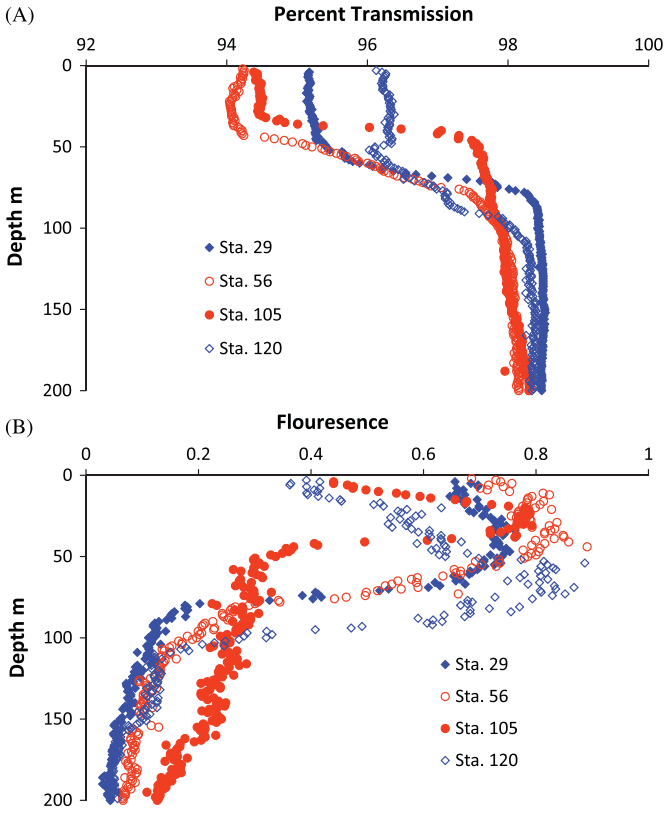

Fig. 3. Shows the upper water column transmissivity (% transmittance) and fluorescence profiles for the near-field stations. For comparison, markers for the downstream stations are red, markers for the upstream stations are blue.

mixed layer followed by ^{234}Th regeneration above 50 m depth (Fig. 4F). It is worth noting that iceberg alley is a region where large icebergs are common. However, none were in the vicinity of our profile collection within the time frame of this study.

The net export of ^{234}Th activity at each site was determined by integrating the difference with the parent over the upper 100 m of the water column. For the purpose of calculation of ^{234}Th export, the system was treated as steady-state. This assumption was based on the consistency of the profiles over the time frame of the experiment (after Savoye et al., 2006) and will be addressed in more detail below. Net export was determined using the steady-state equation:

$$P = \lambda 234_{\mathrm{Th}}(A238_U - A234_{\mathrm{Th}}),$$

where P is the export of ^{234}Th on particulates as disintegrations per minute (dpm) of ^{234}Th meter^{-2}day^{-1}, $\lambda 234_{\mathrm{Th}}$ is the decay constant for ^{234}Th (0.02876 day^{-1}), and $A238_U$ and $A234_{\mathrm{Th}}$ are the activities of ^{238}U and ^{234}Th in units of dpm meter^{-3}. The export of ^{234}Th activity (P) is multiplied by the C/Th from LST collections to determine organic carbon export.

The organic carbon concentration to ^{234}Th activity ratios (C/Th) were determined on LST samples and in samples of fecal pellets collected by depuration of live grazers (Antarctic krill, *Euphausia superba*). Unfortunately, large-volume *in-situ* pumps were not available for this cruise, so size fractions of water column particulates were limited to small-size fractions from Niskin bottle collections. The Niskin samples had very high C/Th, possibly reflecting sampling bias or DOC adsorption (after Buesseler et al., 2006) and were not used for calculation of C export. The highest C/Th was measured for fecal material and water-column particulates, and the lowest was measured in trap material from the LST control site (Sta. 136)(Table 1). The C/Th ratio in LST samples was highest in the near-field samples and lowest for the control samples, differing by approximately a factor of two.

Organic carbon export was calculated at 100 m depth for each site, using net ^{234}Th export (Table 2) and C/Th (Table 1) for concurrent LST deployments and presented in relation to the average LST-measured export at 600 m (Table 2). The 100 m depth integration was used for comparison with other studies in the Southern Ocean. The lowest organic carbon exports were measured for the upstream (< 20-km) site, IB01-120, and the LST control site, Sta. 136, at 16 and 18 mg C m^{-2}d^{-1} respectively, and the highest was measured for the downstream < 20-km site, Sta. 56, at 76 mg C m^{-2}d^{-1}. The average of the iceberg influenced sites was 59 mg C m^{-2}d^{-1}, and the average of the upstream and LST control sites was 17 mg C m^{-2}d^{-1}. The difference is greater than a

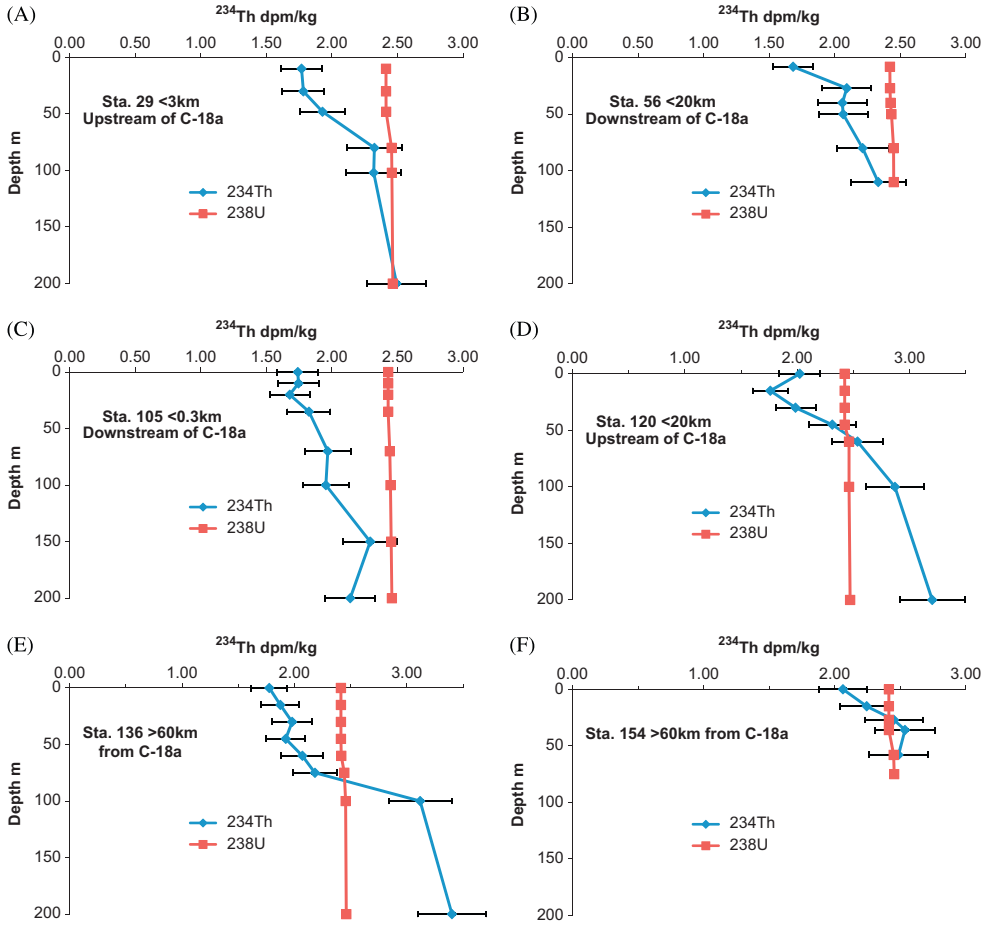

Fig. 4. Fig. 4 presents the water column profiles of ^{234}Th activity (blue diamonds) and the parent ^{238}U activity (red squares) at the six stations.

Table 1
C/Th in LST samples, krill fecal pellets, and water column filtrate.

Sample	C/Th (μg/dpm)	Niskin Water Sample	C/Th (μg/dpm)
LST Sta. 43 Cup 3 Deployed JD77-JD80	36.4 ± 0.8	Sta. 43: 500 m	651 ± 11
LST Sta. 43 Cup 4 Deployed JD77-JD80	35.7 ± 0.8	Sta. 101: 160 m	838 ± 17
LST Sta. 95 Deployed JD87-JD91	30.3 ± 0.6	Sta. 103b: 110 m	816 ± 16
LST Sta. 96 Deployed JD87-JD91	51 ± 1	Sta. 103c: 110 m	874 ± 17
LST Sta. 142 Control Site Deployed JD93-JD97	19.5 ± 0.4	Sta. 163: 160 m	656 ± 13
Krill Fecal Pellets	347 ± 7	Sta. 175: 160 m	731 ± 15

Table 2
Calculated ^{234}Th and Organic Carbon Export . Organic C export for Sta. 29 and Sta. 56 are calculated using the C/Th ratio for the average of two LST samples (Sta. 43 Cup 3 and 4). Organic C export for Sta. 105 and Sta. 120 are calculated using the C/Th ratio for the average of two LST samples (Sta. 95 and Sta. 96). Organic C export for Sta. 136 is calculated using the C/Th ratio for the LST control site samples (Sta. 142).

Sample	^{234}Th Export at 100 m dpm m^{-2}day^{-1} (This study)	Org Carbon Export at 100 m mg C m^{-2}day^{-1} (This study)	Org Carbon Export at 600 m mg C m^{-2}day^{-1} (Smith et al., 2011)
Sta. 29, JD 75 < 3 km upstream of C-18a	1200 ± 100	43 ± 4	5.6 ± 3.1
Sta. 56, JD 79 < 20 km downstream of C-18a	1640 ± 130	76 ± 8	5.6 ± 3.1
Sta. 105, JD 89 < 0.3 km downstream of C-18a	1120 ± 90	57 ± 6	5.6 ± 3.1
Sta. 120, JD 91 < 20 km upstream of C-18a	403 ± 30	16 ± 2	5.6 ± 3.1
Sta. 136, JD 93 LST Control site > 60 km from C-18a	930 ± 60	18 ± 2	2.5
Sta. 154, JD 95 > 60 km from C-18a Iceberg Alley	7 ± 1 integrated to 75 m	No proximal LST C/Th measurement	No proximal LST C export measurement

factor of 3, a difference in ratio similar to that for fluxes measured by the LSTs (Smith et al., 2011). The organic C flux measured by the LSTs at 600 m was about 10% of the organic C flux estimated by ^{234}Th export for both the near-field samples and the control, reflecting approximately 90% regeneration of organic material between 100 and 600 m. Similarly, the ^{234}Th activity export

measured directly in the LST samples averaged ~10% of that leaving the upper 100 m of the water column. The primary production at the near-field sites averaged 275 ± 123 and 184 ± 185 mg C $m^{-2}d^{-1}$ for the control site (Vernet et al., 2011). The inventory of particulate organic carbon (POC) at the near-field sites averaged 1010 ± 203 mg C m^{-2} in the photic zone and 892 ± 107 mg C m^{-2} for the LST control site (Vernet et al., 2011). The calculated carbon export for the upper 100 m was ~21% of the primary production for the near-field sites but only about 10% for the control site. The turnover of the POC inventory (as fraction removed on a daily basis) was 6% for the near-field sites and only 2% for the control site.

4. Discussion

Our model for calculation of ^{234}Th export assumes a system in steady state. An assumption of steady state for a Lagrangian system like a large free-drifting iceberg implies either: 1. Variance induced by the iceberg that is small on a regional scale (e.g. regional steady state); or 2. A persistent area of influence that moves with the iceberg. On the basin scale, the differences between the downstream near-field profiles and the far-field profiles suggest that regional differences are significant in the context of ^{234}Th export and preclude assumption 1 (regional steady state). The difference associated with increased depth of particulate distribution reflects, in part, intensified mixing in the downstream station profiles. The persistence of physical effects (as intensified mixing) supports assumption 2. The area of influence based on measured physical parameters (T and S) included a zone of enhanced vertical mixing extending to a minimum of 20 km downstream from edge of the iceberg (Fig. 2 Sta. 56). The differences between downstream and upstream properties suggest that the area of influence is more intense ahead of the iceberg (Fig. 2). This is consistent with iceberg motion following prevailing currents, but at slower velocities, creating an obstacle in the current. While the upstream station, Sta. 29, did not show strong evidence of enhanced mixing, it was within the zone of physical influence of the iceberg and iceberg grazer community (Smith et al., 2007; Helly et al., 2011; Stephenson et al., 2011; Kaufmann et al., 2011). Thus, Sta. 29 is treated as an iceberg-"influenced" site.

The conditions and persistence of the zone of physical influence were evaluated in greater detail in two concurrent studies during the cruise (Stephenson et al., 2011; Helly et al., 2011). Stephenson et al. (2011) identified mechanisms of enhanced upwelling associated with meltwater entrainment and turbulence. Evidence of enhanced mixing was noted as a reduction and broadening of the temperature minima in the water column proximal to iceberg-18a. (Stephenson et al., 2011). The physical evidence of the water-column disturbance was also measured by reoccupation of an area where C-18a had passed after 10 d (the reoccupation time was determined by logistics). Temperature and salinity anomalies were detectable after 10 d, supporting the view that physically-induced effects on particle distribution (e.g., phytoplankton community size and abundance) are persistent (Helly et al., 2011). These results also support the use of a steady-state model of ^{234}Th export in a Lagrangian system.

We assume a simple conceptual model where the difference in velocity between the iceberg and current generates a plume where ^{234}Th and carbon export conditions persist at near-constant rates as the iceberg moves. We assume that the plume persists significantly longer than time scales for particle dynamics and ^{234}Th adsorption. The conditions leading to a persistent plume are assumed in the case of natural fertilization in proximity to an island or in a region of constant upwelling (e.g., KEOPS study, Blain, 2007), though on a much larger scale than for an individual iceberg. Conditions within the plume approximate steady state, but the steady state assumption fails as the conditions defining the plume decay with distance (or time) from the source. An argument can be made that a large moving iceberg is equivalent to a steady-state plume with a moving source. While the physical data and ^{234}Th deficiency data tend to support the assumption of a moving plume at steady state, logistics precluded a more complete test of this assumption.

4.1. Phytoplankton community at C-18a and carbon export

There are several possible explanations for the differences in calculated organic carbon export in the iceberg influenced sites when compared to Sta. 120 and the LST control site (Sta. 136). One possibility is a phytoplankton particle size effect (after Buesseler, (1998)) leading to lower particulate regeneration and more efficient export in the iceberg influenced samples. This is consistent with the observation of a greater fraction of larger diatoms in the near-field sample collections (Vernet et al., 2011). A second possibility is greater export efficiency associated with particulate aggregation following diatom bloom events (Buesseler, 1998; Shaw et al., 1998), again consistent with observations of relatively higher proportions of large diatoms in the near-field sites. A third possibility is more efficient export associated with a more established grazer community (after Ebersbach and Trull, 2008). There was a higher biomass of grazers in the near-field during Mar-Apr 2009. Elevated densities of krill and salps could have resulted in more efficient packaging and export of organic material (Kaufmann et al., 2011). The third possibility is consistent with observations of established communities associated with free drifting icebergs (Smith et al., 2007).

In the material collected in the LST deployments Sta. 43 and Sta. 96, diatoms were prevalent, with the small diatom *Fragilariopsis nana* and the large species *Corethron pennatum* dominating. Zooplankton and micronekton fecal material was abundant, dominated by euphausiid pellets and strings (Smith et al., 2011). In addition, detrital aggregates were present in collections Sta. 43 and Sta. 96. In the LST control site deployment (Sta. 142) the most diverse distribution of diatoms was observed, though still dominated by *Fragilariopsis nana* and *Corethron pennatum*. In contrast to the other sites, many of the *Corethron pennatum* frustrules at the control site were empty. Ovoid and string fecal material was also present (Smith et al., 2011).

The differences in primary production between the near-field and control sites were relatively small in terms of total primary production (a factor of ~1.5) and do not account for the differences in export measured by the ^{234}Th deficiency method or by the LST's (Vernet et al., 2011). However, the difference in phytoplankton community structure was more pronounced. The abundance of large cells in proximity to the icebergs demonstrates a sharp contrast with the far-field LST control site (Cefarelli et al., 2011). The abundance of large cells would be expected to support more efficient carbon export (Buesseler, 1998) as well as a robust community of grazers (Vernet et al., 2011). The grazers in turn promote packaging of carbon into fast-sinking particles The difference in cell size is thought to be a consequence of upwelling and enhanced nutrient supply induced by the structure of the iceberg.

4.2. Physical effects of C-18a and carbon export.

The physical impact of a relatively large iceberg like C-18a on water-column mixing can exert a significant "bottom up" control on phytoplankton population and ultimately, carbon export. Upwelling of saltier "winter water" is evident in the S profiles of the downstream stations and is accompanied by broadening of the T minimum (Fig. 2, Sta. 56 and Sta. 105). These physical indicators are coincident with lower surface water transmissivity.

Table 3
Comparison of organic carbon exports measured in Southern Ocean Locations.

Location	Sampling Period	Integration Depth (m)	Org Carbon Export mg m^{-2} d^{-1}	Reference	Location
SoFEX Fe fertilization	1/30/02 2/26/02	100	Start 19.2 End 142.6	Buesseler et al., 2005	66°S, 172°E
KEOPS, Kerguelen Plateau, plume	1/19/05 - 2/13/05	100	108-460	Savoye et al., 2008	49°-52°S, 75° 36'E
KEOPS, Reference station	1/19/05 - 2/13/05	100	19.2-57.6	Savoye et al., 2008	50° 37.7"S, 68° -72°
CROZEX, Crozet Plateau	1/05	100	252	Morris et al., 2007	46°S, 52°E
N.W. Weddell Sea Iceberg Influenced	3/17/09 - 4/1/09	100	43-76	This study	61° - 62°S 49° - 52°W
N.W. Weddell Sea Background	4/2/09 - 4/9/09	100	16-18	This study	61° - 62°S 49° - 52°W

Transmissivity data suggest higher particle abundance in surface waters downstream of the icebergs (Fig. 3A). Similarly, the fluorescence data for Sta. 105 indicates a deeper inventory of biogenic material than observed for other near-field stations.

The contrast between the iceberg influenced and far-field ^{234}Th activity profiles in terms of rates of particle sedimentation was evident below 100 m, where regeneration of organic carbon should become important (Fig. 4). While the sampling resolution was not high enough on the deeper segments of the profiles to measure inventories with confidence, the general trends in the deeper profiles contrast sharply. The near-field downstream sites (Sta. 56 and Sta. 105) show deficiency or near-equilibrium levels below 100 m, while the far-field sites show release of ^{234}Th at or above 100 m. Comparison of the profile for the nearest approach to C-18a and the far-field sites provide a striking contrast (Figs. 4C and 4D–F). Biogenic particles appear to be getting deeper in the water column before decomposition (as ^{234}Th regeneration). These observations are consistent with efficient export associated with larger phytoplankton cells and/or efficient packaging by grazers as suggested by Vernet et al. (2011).

4.3. Iceberg grazer community and carbon export

The combination of physical and chemical data demonstrate the potential for large icebergs to impact particulate inventories and rates of particulate export. The hypothesis put forth by Vernet et al. (2011) that packaging of particulates results in rapid sinking is supported by the ^{234}Th profiles from the iceberg affected sites. The lower regeneration of ^{234}Th in the depths directly below the euphotic zone suggests higher particle sinking rates in these waters. This explanation is also consistent with the pronounced differences in the zooplankton grazer and micronekton communities between the near-field and control sites (Kaufmann et al., 2011).

Kaufmann et al. (2011) found that populations of macrozooplankton and micronekton in the near-field to iceberg C-18a in this study and other large icebergs in 2005 were at levels comparable to the most productive regions of the Southern Ocean. The populations were dominated by two species, Antarctic krill (*Euphasia superba*) and salps (*Salpa thompsoni*). Populations of krill were abundant and patchy within a few kilometers of large icebergs. Fecal pellets collected from live Antarctic krill following a depuration experiment had C/Th on the order of 10 times that of the near-field LST material. The implications for ^{234}Th-based carbon exports are that the abundance of krill fecal pellets in sedimenting material results in much higher carbon export for equivalent ^{234}Th export. Likewise, a higher proportion of fast-sedimenting material would result in lower ^{234}Th (and organic C) regeneration immediately below the photic zone. These observations are consistent with iceberg influenced ^{234}Th activity profiles, higher POC turnover rates in the near-field, variability in near-field LST-determined carbon export, and the difference in C/Th in LST material between the near and far-field LST samples. These observations, taken together, indicate the importance of plankton community composition in increasing organic carbon export near free-drifting icebergs.

5. Conclusions

To put the impact of large icebergs on carbon export in context, it is appropriate to compare this system to other sites of iron fertilization in the Southern Ocean. The ^{234}Th deficiency-based export rates in the iceberg influenced sites in this study are ~25% of those measured during CROZEX at the Crozet Archipelago and for the KEOPS experiment above the Kerguelen Plateau (Morris et al., 2007; Savoye et al., 2008), and about 50% lower than those measured for the SOFEX Fe enrichment experiment at the end of the experiment, (Table 3). The unaffected and control sites are similar to those measured for SOFEX and the Keops reference staton (Buesseler et al., 2005; Morris et al., 2007)., The KEOPS, CROZEX, and SoFEX results reflect export during Astral Summer when productivity is higher compared to our Astral Fall study. While the areal impact of a single iceberg is small in the context of the large natural iron fertilization processes, the relatively large numbers of icebergs transiting the region (Stuart and Long, 2011) make this mechanism significant.

Smith et al. (2011) calculated the area of influence of free-drifting icebergs and associated carbon export based on their population at the time of this study. Five major icebergs were detected in the area of study between March and April 2009, with a combined area of 907 km^2. Treating each iceberg as a circle (after Smith et al., 2011) and assuming a 20 km radius extending beyond the iceberg for the area of influence, we can calculate regional carbon export from the upper 100 m of the water column and the difference due to the iceberg influence for the study area. The study area was ~48,000 km^2 and the integrated background (control) carbon export was calculated as 8.2×10^2 metric tons per day. The area of influence for these five icebergs was ~12,000 km^2, 25% of the study area. The difference between the mean iceberg influenced export and the average for the upstream and far-field (LST control) sites was 42 ± 10 mg C $m^{-2}d^{-1}$. The result is an additional $5.2 \pm 1.0 \times 10^2$ metric tons of carbon export per day (below 100 m) associated with increased carbon export efficiency around free-drifting icebergs, a 64% increase for the study area. Assuming 90% regeneration by 600 m yields an increased export of $5.2 \pm 1.0 \times 10^1$ metric tons of carbon per day to that depth. Only about one-third of the extra carbon export can be accounted for by differences in primary production between near-field and control sites. The remaining difference must relate to increased efficiency of carbon export in this unique system.

Acknowledgments

We are grateful to personnel from Raytheon Polar Services and Edison Chouest Offshore, as well as the captain and crew of the RVIB

Nathaniel B. Palmer for their support over the course of this study. Dr. Claudia Benitez-Nelson provided valuable support during the setup, calibration, and operation of the Risø counters as well as numerous discussions during the preparation of this manuscript. Dr. Justina Burns and the Department of Chemistry and Biochemistry Mass Spectrometry Facility at the University of South Carolina provided support for the analysis of samples. Gordon Stephenson and Dr. John Helly provided support for interpretation and presentation of the physical data and mapping. Two anonymous reviewers contributed a number of useful suggestions and comments on the manuscript. Scott Kindelberger provided assistance in the collection and processing of CTD samples. This research was supported by NSF grant OPP-0636319 and the David and Lucile Packard Foundation.

References

Bienfang, P.K., 1984. Size structure and sedimentation of biogenic microparticulates in a subarctic ecosystem. Journal of Plankton Research 6 (6), 985–995.

Blain, S., Queguiner, B., Armand, L., Belviso, S., Bombled, B., Bopp, L., Bowie, A., Brunet, C., Brussaard, C., Carlotti, F., Christaki, U., Corbiere, A., Durand, I., Ebersbach, F., Fuda, J.L., Garcia, N., Gerringa, L., Griffiths, B., Guigue, C., Guillerm, C., Jacquet, S., Jeandel, C., Laan, P., Lefevre, D., Lo Monaco, C., Malits, A., Mosseri, J., Obernosterer, I., Park, Y.H., Picheral, M., Pondaven, P., Remenyi, T., Sandroni, V., Sarthou, G., Savoye, N., Scouarnec, L., Souhaut, M., Thuiller, D., Timmermans, K., Trull, T., Uitz, J., van Beek, P., Veldhuis, M., Vincent, D., Viollier, E., Vong, L., Wagener, T, 2007. Effect of natural iron fertilization on carbon sequestration in the Southern Ocean. Nature 446, 1070–U1071.

Boyd, P.W., 2008. Introduction and Synthesis: implications of large-scale iron fertilization of the oceans. Mar. Ecol. Prog. Ser. Vol. 364, 213–218.

Buesseler, K.O., 1998. The decoupling of production and particulate export in the surface ocean. Glob. Biogechem. Cycles 12, 297–310.

Buesseler, K.O., Andrews, J.E., Pike, S., Charette, M.A., Goldson, L.E., Brzezinski, M.A., Lance, V.P, 2005. Particle export during the Southern Ocean Iron Experiment (SOFeX). Limnology and Oceanography 50, 311–327.

Buesseler, K.O., Benitez-Nelson, C.R., Moran, S.B., Burd, A., Charette, M., Cochran, J.K., Coppola, L., Fisher, N.S., Fowler, S.W., Gardner, W.D., Guo, L.D., Gustafsson, O., Lamborg, C., Masque, P., Miquel, J.C., Passow, U., Santschi, P.H., Savoye, N., Stewart, G., Trull, T., 2006. An assessment of particulate organic carbon to thorium-234 ratios in the ocean and their impact on the application of ^{234}Th as a POC flux proxy. Marine Chemistry 100, 213–233.

Cefarelli, A., Vernet, M., Ferrario, M.E., 2011. Phytoplankton composition and abundance in relation to free-floating Antarctic icebergs. Deep Sea Research II 58 (11-12), 1436–1450.

Chen, J.H., Edwards, R.L., Wasserburg, G.J., 1986. 238U, 234U and 232Th in seawater. Earth Planet. Sci. Lett. 80, 241–251.

Cochran, J.K., Buesseler, K.O., Bacon, M.P., Wang, H.W., Hirschberg, D.J., Ball, L., Andrews, J., Crossin, G., Fleer, A., 2000. Short-lived thorium isotopes (^{234}Th, ^{228}Th) as indicators of POC export and particle cycling in the Ross Sea, Southern Ocean. Deep-Sea Research II 47, 3451–3490.

de Baar, H.J.W, de Jong, J.T.M., Bakker, D.C.E., Loscher, B.M., Veth, C., Bathmann, U., Smetacek, V., 1995. Importance of iron for plankton blooms and carbon dioxide drawdown in the Southern Ocean. Nature (373), 412–415.

de Baar, H.J.W., Boyd, P.W., Coale, K.H., Landry, M.R., Tsuda, A., Assmy, P., Bakker, D.C.E., Bozec, Y., Barber, R.T., Brzezinski, M.A., Buesseler, K.O., Boye, M., Croot, P.L., Gervais, F., Gorbunov, M.Y., Harrison, P.J., Hiscock, W.T., Laan, P., Lancelot, C., Law, C.S., Levasseur, M., Marchetti, A., Millero, F.J., Nishioka, J., Nojiri, Y., van Oijen, T., Riebesell, U., Rijkenberg, M.J.A., Saito, H., Takeda, S., Timmermans, K.R., Veldhuis, M.J.W., Waite, A.M., Wong, C.-S., 2005. Synthesis of iron fertilization experiments: from the Iron Age in the Age of Enlightenment. J Geophys Res-Oceans 110 C09S16.

Ebersbach, F., Trull, T.W., 2008. Sinking particle properties from polyacrylamide gels during the Kerguelen Ocean and Plateau compared Study (KEOPS): Zooplankton control of carbon export in an area of persistent natural iron inputs in the Southern Ocean. Limnol. and Oceanogr. 53, 212–224.

Helly, J.J., Kaufmann, R.S., Stephenson, G.R., Vernet, M., 2011. Cooling, dilution and mixing of ocean water by free-drifting icebergs in the Weddell Sea. Deep Sea Research II 58 (11-12), 1346–1363.

Kaufmann, R.S., Robison, B.R., Reisenbichler, K., Sherlock, R., Osborn, K., 2011. Composition and structure of macrozooplankton and micronekton communities in the vicinity of free-drifting Antarctic icebergs. Deep Sea Research II 58 (11-12), 1469–1484.

Lin, H., Rauschenberg, S., Hexel, C.R., Shaw, T.J., Twining, B.S., 2011. Free-drifting icebergs as sources of iron to the Weddell Sea. Deep Sea Research II 58 (11-12), 1392–1406.

Martin, J.H., Gordon, R.M., Fitzwater, S.E., 1990. Iron in Antarctic waters. Nature 345, 156–158.

Morris, P.J., Sander, R., Turnewitsch, R., Thomalla, S., 2007. ^{234}Th-derived particulate organic carbon export from an island-induced phytoplankton bloom in the Southern Ocean. Deep-Sea Research II 54, 2208–2232.

Murray, A.E., Peng, V., Wagh, P., 2011. Impact of free-drifting icebergs on marine bacterioplankton activity and community structure. Deep Sea Research II 58 (11-12), 1407–1421.

Pike, S.M., Buesseler, K.O., Andrews, J., Savoye, N., 2005. Quantification of Th-234 recovery in small volume seawater samples by inductively coupled plasma-mass spectrometry. J. Radioanal. Nucl. Chem. 263, 355–360.

Pollard, R.T., Salter, I., Sanders, R.J., Lucas, M.I., Moore, C.M., Mills, R.A., Statham, P.J., Allen, J.T., Baker, A.R., Bakker, D.C.E., Charette, M.A., Fielding, S., Fones, G.R., French, M., Hickman, A.E., Holland, R.J., Hughes, J.A., Jickells, T.D., Lampitt, R.S., Morris, P.J., Nedelec, F.H., Nielsdottir, M., Planquette, H., Popova, E.E., Poulton, A.J., Read, J.F., Seeyave, S., Smith, T., Stinchcombe, M., Taylor, S., Thomalla, S., Venables, H.J., Williamson, R., Zubkov, M.V., 2009. Southern Ocean deep-water carbon export enhanced by natural iron fertilization. Nature 457, 577–U581.

Quetin, L.B., Ross, AKD R.M., 1985. Feeding by *Euphausia superba:* Does size matter?. In: Siegfried, W.R., Condy, I? R., Laws, R.W. (Eds.), Antarctic Nutrient Cycles and Food Webs.. Springer, pp. 372–377.

Raiswell, R., Benning, L.G., Tranter, M., Tulaczyk, S., 2008. Bioavailable iron in the Southern Ocean: the significance of the iceberg conveyor belt. Geochemical Transactions 9, 7. doi:10.1186/1467-4866-9-7.

Raiswell, R, Tranter, M, Benning, LG, Siegert, M, De'ath, R, Huybrechts, P, Payne, T., 2006. Contributions from glacially derived sediment to the global iron (oxyhydr)oxide cycle: implications for iron delivery to the oceans. Geochim Cosmochim Acta 70, 2765–2780.

Rodriguez y Baena, A.M., Boudjenoun, R., Fowler, S.W., Juan Miquel, C., Masqué, P., Sanchez-Cabeza, J.-A., Warnau, M., 2008. 234Thbased carbon export during an iceedge bloom: Seaice algae as a likely bias in data interpretation. Earth and Planetary Science Letters 269, 596–604.

Rutgers van der Loeff, M., Sarin, M.M., Baskaran, M., Benitez-Nelson, C., Buesseler, K.O., Charette, M., Dai, M., Gustafsson, O, Masque, P., Morris, P.J., Orlandini, K., Rodriguez y Baena, A., Savoye, N., Schmidt, S., Turnewitsch, R., Vo¨ge, I., Waples, J., 2006. A review of present techniques and methodological advances in analyzing ^{234}Th in aquatic systems. Marine Chemistry 100, 190–212.

Savoye, N., Benitez-Nelson, C., Burd, C., Cochran, A.B., Charette, J.K., Buesseler, M., Jackson, K.O., Roy-Barman, G.A., Schmidt, M., Elskens, M., S., 2006. Th sorption and export models in the water column: A review. Mar. Chem. 100 (3-4), 234–249.

Savoye, N., Trull, T.W., Jacquet, S.H.M., Navez, J., Dehairs, F., 2008. 234Th-based export fluxes during a natural iron fertilization experiment in the Southern Ocean (KEOPS). Deep-Sea Research II 55, 841–855.

Shaw, T.J., Raiswell, R.W., Hexel, C.R., Vu, H.P., Dudgeon, R., Smith, K.L., 2011. Input, Composition, and Potential Impact of Terrigenous material from Free-Drifting Icebergs in the Weddell Sea. Deep Sea Research II 58 (11-12), 1376–1383.

Shaw, T.J., François, R., 1991. A fast and sensitive ICP-MS assay for the determination of ^{230}Th in marine sediments. Geochim. Cosmochim. Acta 55, 2075–2078.

Shaw, T.J., Smoak, J.M., Lauerman, L., 1998. Scavenging of ^{234}Th, ^{230}Th, and ^{210}Pb by particulate matter in the deep waters of the California continental margin. Deep Sea Res., II 45 (763–779), 1998.

Sherlock, R.E., Reisenbichler, K.R., Bush, S.L., Osborn, K.J., Robison, B.H., 2011. Near-field zooplankton, ice-face biota and proximal hydrography of free-drifting Antarctic icebergs. Deep-Sea Research II 58 (11-12), 1457–1468.

Smith, W.O., Lancelot, C., 2004. Bottom-up versus top-down control in phytoplankton of the Southern Ocean. Antarctic Science 16 (4), 531–539.

Smith Jr., K.L., Robison, B.H., Helly, J.J., Kaufmann, R.S., Ruhl, H.A., Shaw, T.J., Twining, B.S., Vernet, M., 2007. Free-drifting icebergs: Hot spots of chemical and biological enrichment in the Weddell Sea. Science 317, 478–482.

Smith, K.L., Sherman, A.D., Shaw, T., Murray, A., Vernet, M., Cefarelli, A.O., 2011. Carbon export associated with free-drifting icebergs in the Southern Ocean. Deep Sea Research II 58 (11-12), 1485–1496.

Stephenson, G.R., Sprintall, J., Gille, S.T., Vernet, M., Helly, J.J., Kaufmann, R.S., 2011. Subsurface melting of a free-floating Antarctic iceberg. Deep Sea Research II 58 (11-12), 1336–1345.

Stuart, K.M., Long, D.G., 2011. Tracking large tabular icebergs using SeaWinds scatterometer. Deep Sea Research II 58 (11-12), 1285–1300.

Vernet, M., Sines, K., Chakos, D., Cefarelli, A.O., Ekern, L., 2011. Impacts on phytoplankton dynamics by free-drifting icebergs in the NW Weddell Sea. Deep Sea Research II 58 (11-12), 1422–1435.

Walsh, J.J., Dieterle, D.A., Lenes, J., 2001. A numerical analysis of carbon dynamics of the Southern Ocean phytoplankton community: the roles of light and grazing in effecting both sequestration of atmospheric CO_2 and food availability to larval krill. Deep-Sea Research Part I—Oceanographic Research Papers 48, 1–48.